MCB
Journals.ASM.org

$p19^{Ink4d}$ Is a Tumor Suppressor and Controls Pituitary Anterior Lobe Cell Proliferation

Feng Bai,[a] Ho Lam Chan,[a] Matthew D. Smith,[c] Hiroaki Kiyokawa,[d] Xin-Hai Pei[a,b]

Molecular Oncology Program, Department of Surgery,[a] and Sylvester Comprehensive Cancer Center,[b] University of Miami Miller School of Medicine, Miami, Florida, USA; Lineberger Comprehensive Cancer Center, University of North Carolina at Chapel Hill, Chapel Hill, North Carolina, USA[c]; Department of Molecular Pharmacology and Biological Chemistry, Northwestern University, Chicago, Illinois, USA[d]

Pituitary tumors develop in about one-quarter of the population, and most arise from the anterior lobe (AL). The pituitary gland is particularly sensitive to genetic alteration of genes involved in the cyclin-dependent kinase (CDK) inhibitor (CKI)–CDK-retinoblastoma protein (Rb) pathway. Mice heterozygous for the *Rb* mutation develop pituitary tumors, with about 20% arising from the AL. Perplexingly, none of the CKI-deficient mice reported thus far develop pituitary AL tumors. In this study, we show that deletion of $p19^{Ink4d}$ (*p19*), a CKI gene, in mice results in spontaneous development of tumors in multiple organs and tissues. Specifically, more than one-half of the mutant mice developed pituitary hyperplasia or tumors predominantly in the AL. Tumor development is associated with increased cell proliferation and enhanced activity of Cdk4 and Cdk6 and phosphorylation of Rb protein. Though Cdk4 is indispensable for postnatal pituitary cell proliferation, it is not required for the hyperproliferative pituitary phenotype caused by p19 loss. Loss of p19 phosphorylates Rb in $Cdk4^{-/-}$ pituitary AL cells and mouse embryonic fibroblasts (MEFs) and rescues their proliferation defects, at least partially, through the activation of Cdk6. These results provide the first genetic evidence that *p19* is a tumor suppressor and the major CKI gene that controls pituitary AL cell proliferation.

The retinoblastoma protein (Rb) family includes three structurally related nuclear phosphoproteins, pRB, p107, and p130, which when hypophosphorylated, negatively regulate the activity of E2F transcription factors to prevent S-phase entry. In mammalian cells, extracellular mitogens induce the expression of D-type cyclins and consequently activate cyclin D and cyclin-dependent kinase 4/6 (CDK4/6) binding, leading to phosphorylation and functional inactivation of Rb proteins. Conversely, inhibition of CDK4/6, resulting from either lack of cyclin D synthesis or binding with CDK inhibitors (CKIs), retains Rb proteins in their growth-suppressive states and prevents G_1-to-S transition. Disruption of this CKI/cyclin D-CDK4/6-pRB/E2F pathway accelerates G_1 cell cycle progression and leads to cancer development (1–3). In fact, *Rb* is frequently mutated and cyclin D and CDK4/6 are frequently amplified or overexpressed in human tumors (1–3), and consistently, mutations inactivating *Rb* (4–7) result in the development of various tumor types in mice.

Mammalian cells express two distinct families of CKIs, the p21 family, including $p21^{Cip1/Waf1}$, $p27^{Kip1}$ and $p57^{Kip2}$ (here p21, p27, p57), and the INK4 family comprising $p16^{Ink4a}$, $p15^{Ink4b}$, $p18^{Ink4c}$, and $p19^{Ink4d}$ (here p16, p15, p18, and p19). Biochemically, CKIs within each family act almost indistinguishably in binding to and regulating CDK enzymes but differ among the families. The p21 family proteins are capable of interacting with multiple CDK-cyclin complexes, whereas the INK4 proteins exclusively bind to and inhibit the kinase activity of CDK4 and CDK6 (1–3). The physiologic significance of evolving a separate family of CKIs and multiple members within each family is presumed to meet the increasing needs for integrating more-intricate and multifaceted cell growth signals into a single cell cycle control machinery. Supporting this notion are the observations that the expression of individual CKI genes is activated selectively by different checkpoint pathways and maintained differentially in discrete adult and senescent tissues. In addition, distinct temporary and spatial patterns are displayed during both *in vitro* cell differentiation and *in vivo* embryonic development (1). Further support for different physiologic functions of individual CKI genes *in vivo* is derived from the genetic analyses of mutant strains of mice with targeted mutation of individual CKI genes. Various phenotypes were observed in these mice, including compromised DNA damage response after inactivation of the *p21* gene (8, 9), increase of tumor development resulting from loss of function of p16 and p15 (10–12), severe developmental defects after *p57* mutation (13), and widespread hyperplastic cell proliferation and organomegaly in p18 and p27 null mice (11, 14–17).

The four INK4 proteins are biochemically very similar, if not indistinguishable (1, 2). Though p19 interacts preferentially with Cdk4 in testis (18) and p18 has greater affinity for CDK6 (1, 2), side-by-side comparisons of complex formation between ectopically overexpressed INK4 with endogenous CDK4 and CDK6 demonstrated a similar affinity of individual INK4 proteins in binding to CDK4 and CDK6 (19). It seems that the differences in the various INK4-CDK interactions are subtle, if not inconsequential, and might have been caused by the analysis of cell types with different endogenous levels of CDK4 and CDK6 (1). The existence of a linear INK4-CDK4/6-Rb-G_1 control pathway in mammalian cells *in vivo* is supported by our previous findings that inactivation of either *p16* or *p18* in mice results in elevated Cdk4 kinase activity and Rb phosphorylation and that the function of p18 in mice is wholly dependent on Cdk4 (20–22).

p16 is frequently mutated in human tumors (23), and muta-

Received 11 October 2013 **Returned for modification** 28 October 2013
Accepted 25 March 2014
Published ahead of print 31 March 2014
Address correspondence to Xin-Hai Pei, xhpei@med.miami.edu.

doi:10.1128/MCB.01363-13

tions inactivating *p16* (10, 12), *p15* (11), or *p18* (11, 15) in mice lead to tumor development, indicating that p16, p15, and p18 are tumor suppressors. p19 is highly and ubiquitously expressed in both fetal and adult tissues (24), and loss or downregulation of p19 is frequently detected in human hepatocellular carcinoma (25), testicular germ cell tumors (26), glioblastoma, leukemia, and lung adenocarcinoma (Oncomine TCGA data set; https://www.oncomine.org/resource/). Paradoxically, disruption of *p19* in mice by insertion of a LacZ-Neo cassette into exon 2 results in a relatively minor phenotype of testicular atrophy with no tumor development (27, 28).

The pituitary gland is a central endocrine organ that controls growth, reproduction, and metabolism. Autopsy studies suggest that pituitary tumors develop in about one-quarter of the population, and most are pituitary anterior lobe (AL) tumors that express and secrete various hormones that contribute to multiple endocrine syndromes (29). The pituitary gland is highly sensitive to genetic alteration of genes in the CKI-CDK-Rb pathway. Proteins involved in regulation of this pathway are altered in nearly all human pituitary tumors (30–35), and Cdk4 is indispensable for postnatal proliferation of the anterior pituitary in mice (36–38). Mice heterozygous for the *Rb* mutation or chimeric for homozygous inactivation of *Rb* are highly predisposed to pituitary tumors (4–7), most of which are in the intermediate lobe (IL). About 20% of *Rb* heterozygous mice develop pituitary AL tumors (6, 34). Interestingly, loss of p27 (14, 16, 17) or p18 (11, 15) in mice leads to pituitary tumor formation predominantly in the IL, and mutations conferring Cdk4 resistance to Ink4 result in the development of pituitary tumors mostly in the AL (39). Perplexingly, none of the CKI-deficient mice reported thus far developed pituitary AL tumors (1, 2, 34). Since p19 is predominantly expressed in the AL of the pituitary (40), we hypothesized a function of p19 in controlling pituitary AL cell proliferation.

In this study, we generated p19 knockout mice by deletion of the *p19* gene from the genome. Our analysis of p19-deficient mice suggests that *p19* is a tumor suppressor and the major CKI gene that controls pituitary AL cell proliferation.

MATERIALS AND METHODS

Gene targeting and generation of mutant mice. The targeting construct was generated to delete a 4.6-kb genomic fragment containing both exons 1 and 2 encoding all 166 amino acid residues of the mouse p19 protein. Briefly, a 16.4-kb mouse genomic DNA fragment spanning the *p19* locus was isolated by PCR from mouse embryonic stem (ES) cell genomic DNA. A LoxP site was introduced downstream of exon 2 by site-directed mutagenesis (Stratagene), and a neomycin (*neo*) resistance gene flanked by LoxP sites was inserted upstream of the promoter region. The linearized targeting construct was electroporated into embryonic day 14 (E14) ES cells that were selected with G418 and ganciclovir. Doubly resistant $p19^{+/NeoFlox}$ clones were screened for homologous recombination events and confirmed by PCR and Southern blot analysis. After transfection of Cre recombinase, $p19^{+/-}$ ES clones with deletion of the *neo* cassette and exons 1 and 2 were screened and identified. Three independent $p19^{+/-}$ ES clones were injected into C57BL/6 blastocysts, and chimeric mice were crossed with C57BL/6 mice to generate $p19^{+/-}$ heterozygotes. $p19^{+/-}$ mice were backcrossed for six generations with C57BL/6 mice before being used for this study. $p19^{+/-}$ mice were intercrossed to generate $p19^{-/-}$ mice, and successful deletion of *p19* was confirmed by PCR and Southern blotting. p19 deficiency was further confirmed by Western blotting.

The generation of *Cdk4*, *p18*, and *p18*; *Cdk4* mutant mice has been described previously (15, 21, 38). Mice deficient for *p19* were bred to the mice heterozygous for *Cdk4* to create double-heterozygous mice, which were then intercrossed to generate *p19*; *Cdk4* double-knockout mice. Animals were genotyped by PCR and monitored as described previously (15, 21, 38). Cohorts were housed and analyzed in a common setting, and littermate controls were used for all experiments as indicated. All animal studies were approved by the Institutional Animal Care and Use Committee (IACUC) at the University of North Carolina and at the University of Miami.

Analysis of fertility and diabetes. Two- to four-month-old $p19^{-/-}$, $Cdk4^{-/-}$, $p19^{-/-}$; $Cdk4^{-/-}$, or wild-type (WT) C57BL/6 male and female mice were individually housed for 21 days with a paired female or male mouse of a similar age. Females were then separated from the males and allowed to rest for 21 days. A female was considered fertile if she gave birth to pups, and a male was fertile if the female in the same cage gave birth to pups. Litter size was determined by counting pups. Blood glucose levels were monitored in the morning (8 to 10 a.m.) by using an automatic glucose monitor (Glucometer Elite; Bayer). Each mouse was analyzed twice for blood glucose on two consecutive days.

Tumor analysis, histopathology, and IHC. For the determination of spontaneous tumor incidence, WT and *p19* mutant mice with visible tumors, exhibiting morbidity, weight loss, or paralysis were sacrificed. The remaining surviving mice were sacrificed at 27 months of age. A full autopsy was performed, and tissues were fixed and histologically examined by two pathologists after hematoxylin and eosin (H&E) staining. The survival rate was calculated by the Kaplan-Meier method with Prism software (version 5.01; GraphPad Software), and statistical significance was assessed with Wilcoxon's log rank test. Histopathology and immunohistochemistry (IHC) were performed as described previously (21). Primary antibodies used were as follows: p-Rb-S608 (Cell Signaling); prolactin (PRL), growth hormone (GH), and follicle-stimulating hormone (FSH) (Thermo Scientific); Cdk6 (generated and characterized in the lab [41]); and Ki67 (Novartis). Immunocomplexes were detected using the Vectastain Elite ABC peroxidase kit (Vector Laboratories).

MEFs and flow cytometry procedures. Primary MEFs were isolated from E13.5 embryos. Early-passage MEFs (<passage 4) from individual embryos were plated in 100-mm plates and incubated in Dulbecco's modified Eagle medium (DMEM) plus 10% fetal bovine serum (FBS). For serum starvation, asynchronous cultures at approximately 50% confluence were washed with phosphate-buffered saline (PBS) and serum starved in DMEM containing 0.1% FBS for 72 h. Cells were restimulated by addition of DMEM with 10% FBS. For bromodeoxyuridine (BrdU) labeling, MEFs were grown in media with or without serum containing 10 μM BrdU for 1 h. Nuclei were isolated following trypsinization and fixation with 95% ethanol by incubation in 0.08% pepsin (Sigma) in 0.1 N HCl for 20 min at 37°C. Nuclear DNA was denatured by incubating in 2 N HCl for 20 min at 37°C followed by neutralization with $Na_2B_4O_7$, pH 8.5. Incorporated BrdU was detected using anti-BrdU-fluorescein isothiocyanate (FITC) (1:10 dilution; Becton, Dickinson) in 10 mM HEPES (pH 7.3), 150 mM NaCl, 4% FBS, and 0.5% Tween 20. MEFs were then harvested and resuspended in PBS containing 1% FBS, incubated with propidium iodide (PI; 5 $\mu g/ml^{-1}$), and RNase A (0.1 mg/ml^{-1}) for 30 min at 37°C. The samples were analyzed with a FACScan or LSRFortessa (Becton, Dickinson), and the data were processed with Summit (version 3.0; BD Biosciences) and Kaluza (version 1.2; Beckman Coulter) software.

RNA interference (RNAi). A pair of complementary small interfering RNA (siRNA) oligonucleotides targeting nucleotides 209 to 229 (AAGA UGCCUCCGGUACUAGUC) relative to the translation initiation codon of mouse p19 were synthesized at Dharmacon (Lafayette, CO). Early-passage wild-type MEF cells (<passage 3) were seeded at 20 to 30% confluency in a 60-mm plate and transfected twice with siRNA at 24 and 48 h after initial seeding with either single-sense strand siRNA oligonucleotide or annealed siRNA duplex. A 120-μl volume of Opti-MEM was mixed with 30 μl Oligofectamine reagent for 8 min and incubated with a mixture containing 30 μl siRNA and 500 μl Opti-MEM for 20 min at room temperature. An additional 320 μl of Opti-MEM was added to the mixture, and the entire 1,000 μl was added for transfection into each

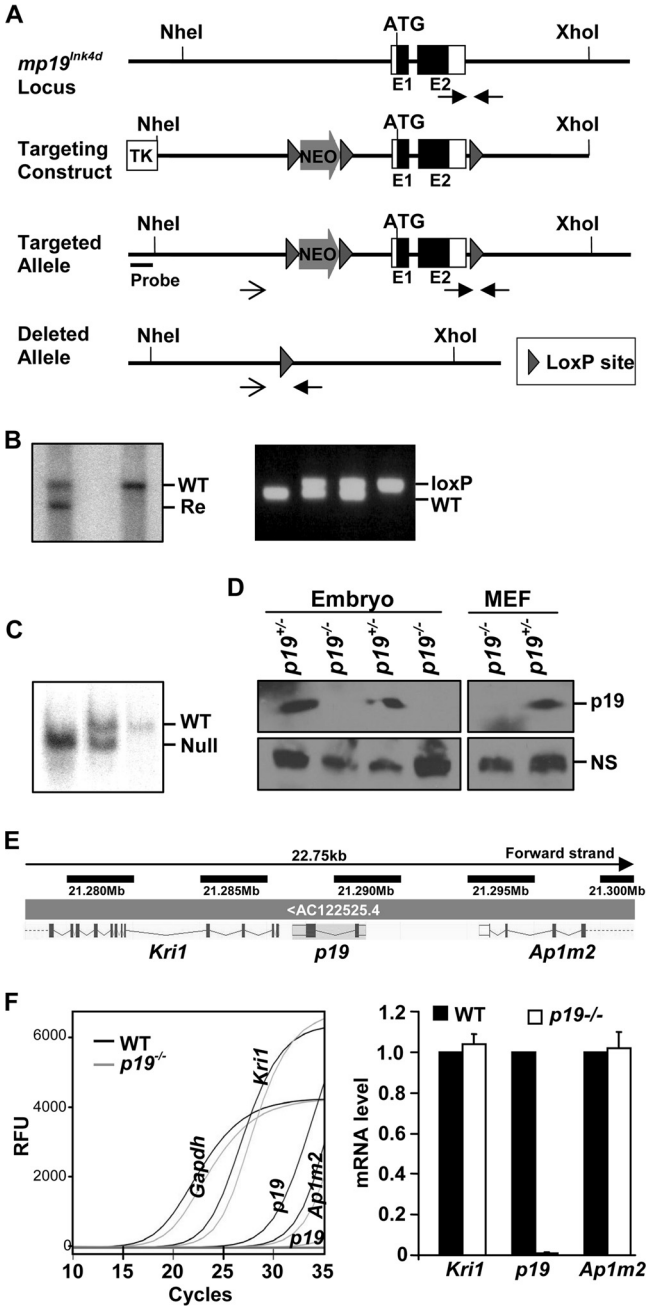

FIG 1 Targeted deletion of *p19* locus. (A) Schematic presentation of the mouse *p19* locus. A 16.4-kb fragment of mouse genomic DNA, spanning both exons, was amplified by PCR from mouse ES cell genomic DNA and verified by DNA sequencing. LoxP sites were inserted at the indicated sites. (B) After electroporation into E14 ES cells, G418 and ganciclovir doubly resistant clones were screened for homologous recombination by PCR and Southern blotting. Re, recombined allele. (C) Targeted $p19^{+/NeoFlox}$ ES cells were transfected with cytomegalovirus (CMV)-Cre vector. Deletion of NEO and exons 1 and 2 ($p19^{+/-}$) was screened by Southern blotting. Three independent $p19^{+/-}$ ES clones were injected into C57BL/6 blastocysts. Germ line-transmitted agouti pups were intercrossed, and the genomic DNA from the progeny ears was analyzed by Southern blotting. (D) p19 deficiency was confirmed by Western blotting of protein lysates from E16 embryos and MEFs of the indicated genotype. (E) Schematic map of genomic structure of mouse chromosome 9 spanning the *p19* locus. A 22.75-kb region on mouse chromosome 9 spanning the *p19* locus is shown based on the assembly by NCBI. Three genes are identified in this region. (F) The expression of genes neighboring the *p19* locus was examined by qRT-PCR. RNA from asynchronously growing MEFs was extracted and analyzed for the expression of the genes indicated. Real-time amplification curves for *Kri1*, *p19*, and *Ap1m2* from cDNA of WT and $p19^{-/-}$ MEFs are shown (left). Results represent the means ± standard deviations (SD) from triplicates of each of the three independent MEF lines (right). Expression of *p19* was not detected, and that of *Kri1* and *Ap1m2* was unchanged in $p19^{-/-}$ MEFs. RFU, relative fluorescence units.

60-mm plate. Twenty-four hours after the second transfection, RNA or protein was harvested for further analysis.

qRT-PCR. Total RNA was extracted using the RNeasy minikit (Qiagen), and cDNA was synthesized with random hexamers by the SuperScript III first-strand synthesis system (Invitrogen). The cDNA was added to a quantitative reverse transcription-PCR (qRT-PCR) mixture that contained 1× SYBR green PCR master mix (Applied Biosystems) and 70 nM gene-specific primers. Assays were performed in triplicate on a CFX96 real-time PCR detection system (Bio-Rad). The expression level of each gene was normalized with GAPDH (glyceraldehyde-3-phosphate dehydrogenase). The specific PCR primer sequences are available upon request.

Immunoprecipitation and Western, Southern, and Northern blots. Tissue or MEF lysates were prepared as previously reported (15, 21). Antibodies to Rb (BD Pharmingen), p19, and tubulin (Santa Cruz), as well as horseradish peroxidase (HRP)-protein A (Invitrogen) were purchased commercially. Antibodies to Cdk4, Cdk6, and cyclins D1, D2, and D3 (Cyc D1, D2, and D3) were described previously (41–43). The procedures for immunoprecipitation and Western and Southern blotting were performed as described previously (41, 43, 44). For Northern blot analysis, MEF cells at early passage were serum deprived (0.1% FBS) for 3 days and released from quiescence by serum stimulation (10% FBS). Total RNA was prepared from cells at different time points after serum stimulation as well as from an asynchronized cell population as indicated. RNA samples were resolved on a 1% agarose gel, transferred to a nitrocellulose filter, and hybridized with a probe derived from full-length mouse p19 cDNA. The blot was then stripped and rehybridized with a mouse Gapdh probe.

Kinase assay. Kinase assays were performed using the ADP-Glo kinase assay kit (Promega). Protein lysate from MEFs or pituitary tissues pooled from three mice of the same genotype at 1 year of age was immunoprecipitated with 1 μg of Cdk4 and Cdk6 antibodies, and rabbit IgG was used as the control. After overnight incubation, protein A/G-agarose beads (Santa Cruz) were added, incubated for 1 h, and washed three times with lysis buffer followed by two washes in kinase reaction buffer (50 mM HEPES, 10 mM $MgCl_2$, 5 mM $MnCl_2$, 10 μM ATP, and 1 mM dithiothreitol [DTT]) (45). Beads were then resuspended in 10 μl kinase reaction buffer and incubated for 1 h at 30°C with glutathione *S*-transferase (GST)–Rb (45). The reaction was terminated by adding 5 μl ADP-Glo reagent, and the mixture was incubated for 40 min at room temperature followed by addition of 10 μl kinase detection reagent and incubation at room temperature for 30 min. Luminescence was determined using a $20/20^n$ luminometer (Turner Biosystems). Alternatively, for detection of kinase activity by Western blotting, Laemmli sample buffer was added to the completed kinase reaction mixture and a phosphothreonine-specific antibody (Cell Signaling) was used to detect phosphorylated Rb.

RESULTS

Targeted deletion of the mouse *p19* gene. We deleted the mouse *p19* gene by targeted homologous recombination. We made a targeting construct in which a 4.6-kb genomic fragment containing both exons 1 and 2 that encodes the full-length p19 protein was flanked by LoxP sites (Fig. 1A). The linearized targeting construct was electroporated into ES cells, and G418 and ganciclovir doubly resistant clones were screened for homologous recombination by Southern blotting and PCR (Fig. 1B). Targeted $p19^{+/NeoFlox}$ ES cells were transfected with an expression vector encoding Cre re-

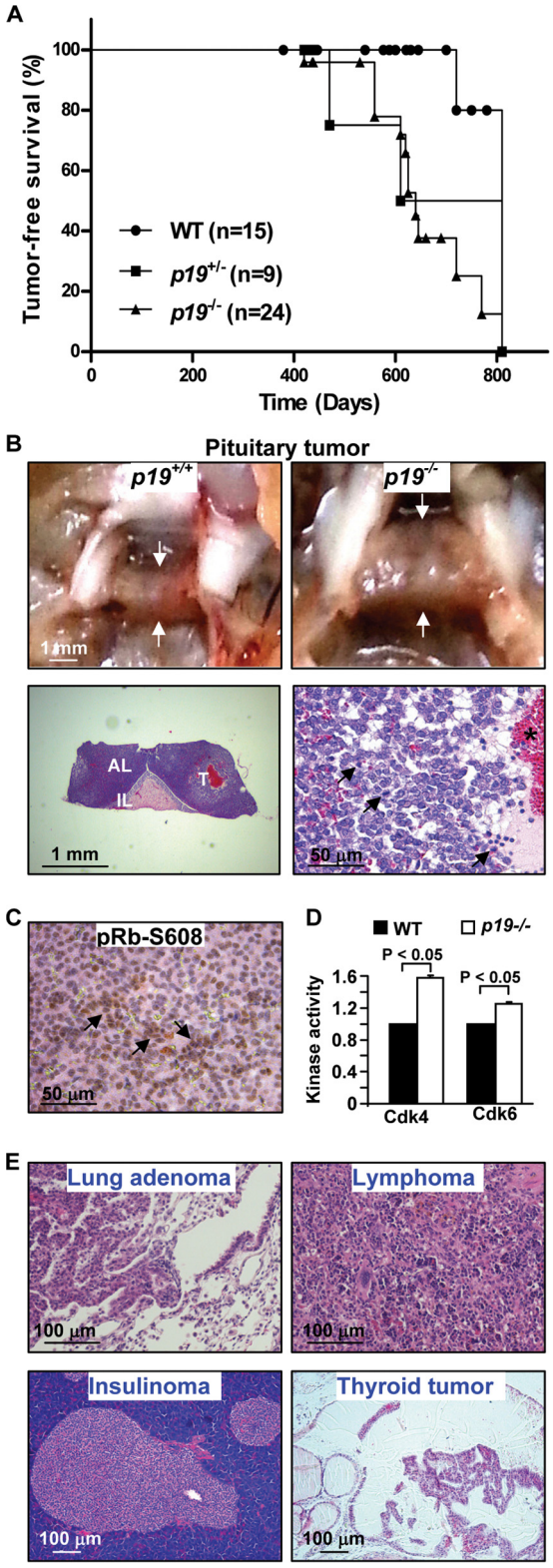

FIG 2 *p19* mutant mice develop spontaneous tumors. (A) Tumor-free survival curve of WT and *p19* mutant mice. (B) Pituitaries from 1-year-old WT and $p19^{-/-}$ mice (top). A pituitary tumor from a 16-month-old $p19^{-/-}$ mouse was stained with H&E and is shown at low (bottom left) and high (bottom right) magnifications. Note the tumor (T) in the anterior lobe. Mitotic cells and blood lake in the tumor are indicated by the arrows and asterisk, respectively. AL, anterior lobe; IL, intermediate lobe. (C) Representative immunostaining of pituitary anterior lobe tumors from $p19^{-/-}$ mice with an antibody against pRb-S608. Positive cells are indicated. (D) Kinase activity associated with Cdk4 and Cdk6 in pituitaries of 1-year-old mice. Three pituitaries from mice of each genotype were pooled for analysis. The results shown are the means ± SD of experiments in triplicate. Statistical significance was calculated using Student's *t* test. (E) Other representative tumors developed in $p19^{-/-}$ mice.

combinase, and $p19^{+/-}$ ES clones that had *neo* and exons 1 and 2 removed were screened and isolated by PCR and Southern blotting. Three independent $p19^{+/-}$ ES clones were injected into blastocysts to generate mutant mice (Fig. 1C and data not shown). Offspring from three independent ES lines were later shown to be phenotypically indistinguishable. p19 deficiency was confirmed by Western blotting and RT-PCR from $p19^{-/-}$ E16 embryos and mouse embryonic fibroblasts (Fig. 1D and F). We then determined the expression of two genes neighboring the *p19* locus, one from each adjacent side (Fig. 1E). We found that mRNA expression of *Kri1*, a gene upstream of *p19*, and *Ap1m2*, a gene downstream of *p19*, was unchanged, whereas the expression of *p19* was undetectable in $p19^{-/-}$ MEFs and embryos (Fig. 1F and data not shown). These results further confirm that the targeting strategy specifically disrupted the *p19* gene without affecting the expression of its neighbor genes.

***p19* mutant mice develop spontaneous tumors.** The $p19^{-/-}$ mice were produced in Mendelian ratios without significant developmental defects. The body weights of both male and female $p19^{-/-}$ mice were indistinguishable from those of WT mice (see Fig. 4A). Though the testes of $p19^{-/-}$ male mice were slightly smaller than those of WT mice, p19-deficient males were fertile, which is in agreement with previous findings (27, 28, 40). After monitoring a cohort of 24 $p19^{-/-}$, 9 $p19^{+/-}$, and 15 wild-type mice for 27 months, we found that 14 (58.3%) $p19^{-/-}$ and 3 (30%) $p19^{+/-}$ mice spontaneously developed tumors, whereas only 2 (13.3%) WT mice displayed tumors at a similar age (Fig. 2A and Table 1). The wide tumor spectrum of $p19^{-/-}$ and $p19^{+/-}$ mice included pituitary and lung adenomas, lymphomas, hemangiosarcoma, thyroid cancer, and insulinoma (Fig. 2B and E and Table 1). Both $p19^{-/-}$ and $p19^{+/-}$ mice had a significantly decreased tumor-free life span compared with WT controls ($P = 0.0058$ for WT versus $p19^{-/-}$ and $P = 0.0219$ for WT versus $p19^{+/-}$). The mean tumor-free survival times for $p19^{-/-}$, $p19^{+/-}$, and WT mice were 640, 710, and 810 days, respectively (Fig. 2A). In addition, *p19* mutant mice were also predisposed to developing pituitary and pancreatic islet hyperplasia as well as ovarian cysts (Table 1). Taken together, these results reveal a function of *p19* in tumor suppression.

Loss of *p19* leads to a hyperproliferative phenotype in pituitary AL. Upon close examination of *p19* mutant mice, we found that, surprisingly, $p19^{-/-}$ pituitaries, the AL in particular, were larger than the WT organ at all ages after 3 months and that 30% (3/9) of $p19^{+/-}$ and 58% (14/24) of $p19^{-/-}$ mice developed hyperplasia or adenoma in the pituitary (Fig. 2A and B, Fig. 3, and Table 1) after 1 year of age. Nearly all pituitary hyperproliferative phenotypes in *p19* mutant mice were detected in the AL, unlike those of *p18* mutant mice, which are observed mostly in the IL (15). We examined cell proliferation in $p19^{-/-}$ pituitaries using the proliferation marker Ki67. We found that there was increased cell proliferation in $p19^{-/-}$ pituitaries, particularly in the lesions with hyperplasia or adenoma, compared to age-matched WT

TABLE 1 Pathology of *p19* mutant mice

Organ[a] and pathology	No. of mice displaying indicated clinical sign		
	WT ($n = 15$)	$p19^{+/-}$ ($n = 9$)	$p19^{-/-}$ ($n = 24$)
Pituitary			
Hyperplasia			
AL	0	2	11
IL	0	0	3[b]
Adenoma			
AL	0	1	3
IL	0	0	0
Lung			
Hyperplasia	0	0	1
Adenoma	1	1	6
Pancreatic islet			
Hyperplasia	0	1	4
Insulinoma	0	0	1
Ovary			
Normal	5	6	8
Cyst	0	0	6
Other tumors			
Lymphoma	1	1	3
Sarcoma	0	0	1
Thyroid tumor	0	0	1
No. of mice with tumor	2	3	14[c]

[a] IL, intermediate lobe; AL, anterior lobe.
[b] All three mice developed hyperplasia in both IL and AL.
[c] One mouse developed lung adenoma and lymphoma simultaneously.

counterparts (5.1% ± 2.2% versus 1.6% ± 0.5% in 4-month-old pituitaries [Fig. 3 and data not shown]). As determined microscopically by their localization in the glands, the majority of the proliferating cells in $p19^{-/-}$ pituitaries were in the AL. We then directly examined the status of Ser608 phosphorylation of Rb, the site that is preferentially phosphorylated by the targets of p19, CDK4, and CDK6 (46–48). A visible and consistent increase of pRb-Ser608 phosphorylation was detected in normal $p19^{-/-}$ pituitary ALs (6.9% ± 2.4% in $p19^{-/-}$ versus 3.4% ± 1.5% in WT [Fig. 3]) and in $p19^{-/-}$ AL hyperplasias and adenomas (Fig. 2C), supporting the activation of Cdk4 and/or Cdk6. These data are also consistent with the previous finding that p19 is predominantly expressed in the AL of pituitary (40). We then determined the kinase activity of Cdk4 and Cdk6 using GST-Rb as the substrate. We found that Cdk4 and Cdk6 kinase activity increased 1.5- and 1.3-fold in p19 null pituitaries in comparison with WT organs (Fig. 2D), confirming the activation of Cdk4 and Cdk6 by p19 loss in the pituitary. Finally, we performed immunohistochemistry (IHC) and confirmed that there were proportionally greater numbers of prolactin (PRL)-, growth hormone (GH)-, and follicle-stimulating hormone (FSH)-expressing cells in $p19^{-/-}$ pituitaries than in WT counterparts (PRL-positive cells, 23.1% ± 6.6% in $p19^{-/-}$ versus 16.3% ± 5.1% in WT; FSH-positive cells, 10.8% ± 4.3% in $p19^{-/-}$ versus 6.9% ± 2.8% in WT [Fig. 3 and data not shown]). Taken together, these results demonstrate that *p19* deficiency stimulates Cdk4 and Cdk6 activity toward Rb protein in pituitary AL cells, increasing their proliferation at an early age and driving them from hyperplasia to tumor.

Cdk4 is not required for the development of a hyperproliferative phenotype in $p19^{-/-}$ pituitaries. The growth-suppressive function of p19 in multiple tissues, particularly in the pituitary AL, prompted us to determine whether the role of p19 in tumor suppression, like that of p18, is dependent on Cdk4. To this end, we generated *p19 Cdk4* double mutant mice. At birth, WT, $Cdk4^{-/-}$, $p19^{-/-}$, and $p19^{-/-}$; $Cdk4^{-/-}$ mice appeared indistinguishable (data not shown). Soon after birth, however, various growth abnormalities were grossly apparent in $Cdk4^{-/-}$ and $p19^{-/-}$; $Cdk4^{-/-}$ mice. $p19^{-/-}$ female mice were slightly bigger and heavier than WT animals (Fig. 4A), and most $p19^{-/-}$ mice lived for up to 2 years, at which time they developed various tumors (Table 1 and Fig. 2A). In contrast, most, if not all, $Cdk4^{-/-}$ mice died early in life (<6 months) as previously reported (38, 49). Loss of *p19* had no significant effect on the postnatal mortality caused by *Cdk4* loss, and no $p19^{-/-}$; $Cdk4^{-/-}$ ($n = 22$) (data not shown) animal lived beyond 9 months. The body weights of $Cdk4^{-/-}$ and $p19^{-/-}$; $Cdk4^{-/-}$ mice were indistinguishable and lower than those of WT or $p19^{-/-}$ mice (Fig. 4A). Thus, loss of *Cdk4* led to growth retardation that was not rescued by *p19* loss.

While $Cdk4^{-/-}$ pituitaries in adult mice, as reported, were extremely hypoplastic (Fig. 3), $p19^{-/-}$; $Cdk4^{-/-}$ pituitaries were slightly bigger than WT pituitaries at a similar age and were significantly bigger than $Cdk4^{-/-}$ counterparts (Fig. 3). $p19^{-/-}$; $Cdk4^{-/-}$ pituitaries, AL in particular, displayed relatively normal histology as observed in WT mice (Fig. 3), indicating that Cdk4 is not required for pituitary development in p19 null mice and that loss of p19 rescues AL hypoplasia induced by Cdk4 loss. Because of early death of $p19^{-/-}$; $Cdk4^{-/-}$ mice from diabetes (see below), we were unable to demonstrate that loss of *Cdk4* would prevent the development of pituitary hyperplasia and adenomas in older $p19^{-/-}$ mice.

To determine the cellular basis of functional independency of *p19* on *Cdk4* in pituitary development, we performed IHC analysis for pituitaries. In $Cdk4^{-/-}$ pituitaries, Ki67-positive cells were barely detectable in both the AL and IL (0.3% ± 0.1%), whereas Ki67-positive cells were moderately increased in $p19^{-/-}$; $Cdk4^{-/-}$ pituitaries—particularly in the AL—relative to WT counterparts (2.3% ± 0.8% in $p19^{-/-}$; $Cdk4^{-/-}$ versus 1.6% ± 0.5% in WT mice [Fig. 3]). Consistently, we detected a significant decrease of pRb-Ser608 phosphorylation in $Cdk4^{-/-}$ pituitary AL (0.5% ± 0.2%) and a drastic increase in $p19^{-/-}$; $Cdk4^{-/-}$ counterparts compared with WT (7.3% ± 3.5% in $p19^{-/-}$; $Cdk4^{-/-}$ versus 3.4% ± 1.5% in WT mice [Fig. 3]). This result indicates that loss of Cdk4 does not abolish the hyperproliferative phenotype in $p19^{-/-}$ pituitaries and loss of p19 rescues pituitary AL hypoplasia caused by Cdk4 deficiency, suggesting that the development of a hyperproliferative phenotype in $p19^{-/-}$ pituitaries does not require Cdk4. Because Ser608 of Rb protein is preferentially phosphorylated by CDK4 and CDK6, the only two CDKs identified thus far as downstream targets of p19 in the regulation of Rb, the increase of pRb-Ser608 phosphorylation and proliferation in $p19^{-/-}$; $Cdk4^{-/-}$ AL cells suggests that Rb phosphorylation in $Cdk4^{-/-}$ pituitaries, when p19 is lost, is likely through activation of Cdk6. To corroborate this point, we then determined the expression of Cdk6 in the pituitary. We detected that Cdk6 was predominantly expressed in AL cells and loss of either Cdk4 or p19, or both, did not significantly affect the Cdk6 expression pattern (Fig. 3). This result suggests an unidentified role of Cdk6 in pituitary anterior lobe development.

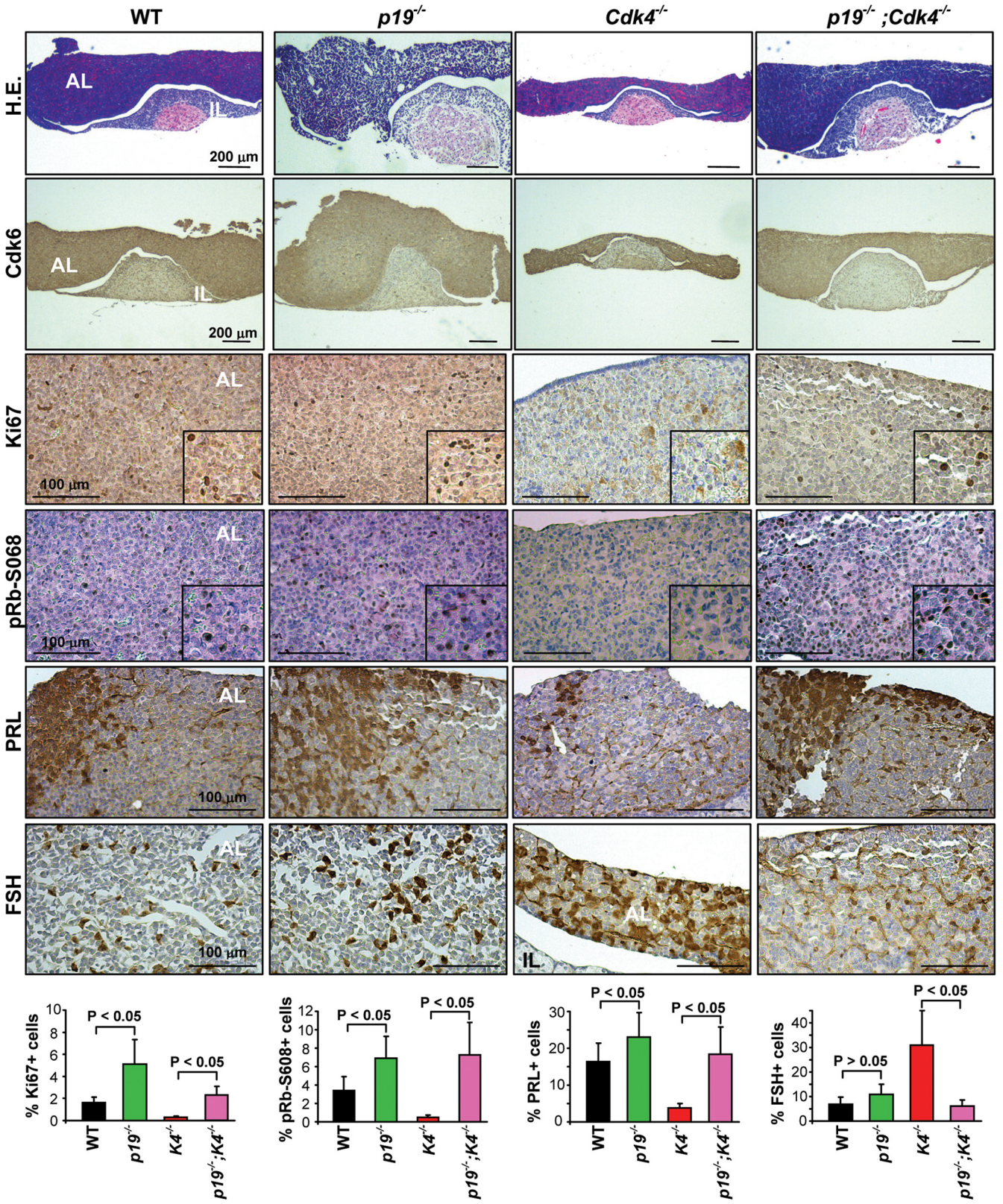

FIG 3 Characterization of pituitaries from mutant mice. Pituitaries from the indicated genotypes were stained with H&E, Ki67, pRb-S608, Cdk6, PRL, and FSH. Insets show magnified representative cells. All pituitaries were derived from mice at 3 to 4 months of age, except one $p19^{-/-}$ pituitary stained with Cdk6 that was from a 16-month-old mouse showing the specific expression of Cdk6 in the AL of old mice. The percentages of Ki67-, pRb-S608-, PRL-, and FSH-positive cells were calculated from 800 to 1,400 cells situated only in the AL. Results represent the means ± SD of three animals per group. Statistical significance was calculated using Student's *t* test.

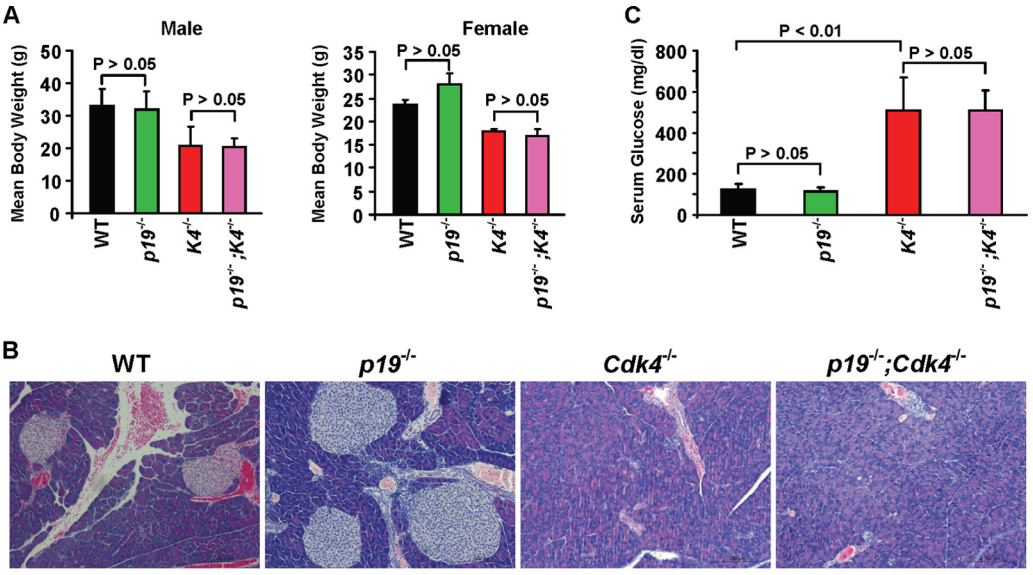

FIG 4 Loss of p19 did not rescue the decreased body weight and diabetes of Cdk4-deficient mice. (A) Mean body weights from male and female mice of different genotypes at 4 months of age were compared. Three to five mice from each genotype were weighed. SD bars are indicated. (B) H&E staining of pancreatic sections from mice of different genotypes at 4 months of age. (C) Glucose levels in sera of 3- to 4-month-old mice were determined. Data were derived from three or four mice from each genotype. SD bars are indicated. Statistical significance was calculated using Student's *t* test.

To determine which particular cell lineage in pituitary AL was affected by *p19* or/and Cdk4 loss, we also performed IHC and found that $Cdk4^{-/-}$ pituitaries displayed markedly decreased numbers of PRL- and GH-expressing cells with proportionally increased numbers of FSH-expressing cells relative to WT (PRL-positive cells, 3.8% ± 1.2% in $Cdk4^{-/-}$ versus 16.3% ± 5.1% in WT mice; FSH-positive cells, 30.9% ± 14% in $Cdk4^{-/-}$ versus 6.9% ± 2.8% in WT mice [Fig. 3 and data not shown]), confirming hypoplasia of the lactotroph and somatotroph but not gonadotroph induced by Cdk4 loss (37, 50). Because a hypoplastic lactotroph is responsible for the defective luteal function and female infertility of Cdk4 null mice and FSH plays an important role in fertility of male mice, we then focused our study on PRL- and FSH-expressing cells. We found that the numbers of PRL-expressing cells in $p19^{-/-}$; $Cdk4^{-/-}$ pituitaries were slightly greater than in the WT but were significantly more than in $Cdk4^{-/-}$ counterparts (PRL-positive cells, 18.3% ± 7.1% in $p19^{-/-}$; $Cdk4^{-/-}$ mice, 16.3% ± 5.1% in WT, and 3.8% ± 1.2% in $Cdk4^{-/-}$ [Fig. 3]). Interestingly, the number of FSH-expressing cells in $p19^{-/-}$; $Cdk4^{-/-}$ pituitaries was less than in $Cdk4^{-/-}$ pituitaries but was comparable with the number in WT counterparts (6.1% ± 2.5% in $p19^{-/-}$; $Cdk4^{-/-}$, 6.9% ± 2.8% in WT, and 30.9% ± 14% in $Cdk4^{-/-}$ mice [Fig. 3]). These results indicate that p19-deficient lactotrophs do not require Cdk4 for development and loss of p19 rescued hypoplasia of the lactotroph caused by Cdk4 deficiency.

Cdk4 is required for development of a hyperproliferative phenotype in $p19^{-/-}$ pancreatic islets. $p19^{-/-}$ pancreatic islets were bigger than WT counterparts at early ages, and $p19^{-/-}$ mice developed hyperplasia (4 of 24) and insulinoma (1 of 24) after 1 year of age, though $p19^{-/-}$ mice displayed normoglycemia (Fig. 4B and C). In contrast, $Cdk4^{-/-}$ mice developed diabetes with hyperglycemia around 7 weeks of age, which was persistent throughout their life, and the $Cdk4^{-/-}$ pancreatic islets were significantly smaller than the WT islets (Fig. 4) (21, 38, 49). Pancreatic phenotypes of $p19^{-/-}$; $Cdk4^{-/-}$ mice were very similar to those of $Cdk4^{-/-}$ mice: islets were sparsely located, and the number and size of islets were comparable to those of $Cdk4^{-/-}$ mice (Fig. 4B). Consistent with the defects in pancreatic islets, $p19^{-/-}$; $Cdk4^{-/-}$ mice also developed diabetes with serum glucose levels comparable to those of $Cdk4^{-/-}$ mice (Fig. 4C). IHC revealed an increase of Ki67-positive cells in $p19^{-/-}$ islets and a significant decrease of Ki67-positive cells in both $p19^{-/-}$; $Cdk4^{-/-}$ and $Cdk4^{-/-}$ counterparts (data not shown). These results indicate that p19 suppresses pancreatic islet cell proliferation and loss of *p19* does not rescue defective islet cell proliferation caused by *Cdk4* loss. Instead, loss of Cdk4 abolishes the hyperplastic growth of pancreatic islets caused by *p19* deletion. These results suggest that the function of p19 in islet proliferation, like that of p18 (21), is also dependent on Cdk4.

Deletion of *p19* rescues defective luteal function and infertility of *Cdk4* null female mice. Pituitary lactotroph dysfunction is responsible for the defective luteal function in Cdk4-deficient mice (37, 50). Since deletion of *p19* rescued hypoplasia of lactotroph caused by Cdk4 deficiency, we then speculated that p19 deficiency may also rescue $Cdk4^{-/-}$ defective luteal function. To test this hypothesis, we examined the ovaries of the mice. As previously reported (21, 38, 49) and also shown in Fig. 5A, adult $Cdk4^{-/-}$ ovaries at 4 months of age display very few corpora lutea (CL)—at most one CL in each ovary. However, most ovaries from WT, $p19^{-/-}$, and $p19^{-/-}$; $Cdk4^{-/-}$ female mice formed one or two CL in each ovary at a similar age, confirming that loss of p19 rescues lactotroph hypoplasia in Cdk4-deficient pituitaries, resulting in normal luteal function.

The defective PRL production and luteal function caused by hypoplasia of lactotroph are responsible for the infertility of female Cdk4 null mice (37, 50). Loss of p19 rescued $Cdk4^{-/-}$ lactotroph hypoplasia and defective luteal function, suggesting that $p19^{-/-}$; $Cdk4^{-/-}$ female mice may be fertile. To test the fertility of the mutant mice, 10 $p19^{-/-}$ female mice were mated for 21 days with either WT or $p19^{-/-}$ male mice separately. More than 60% of

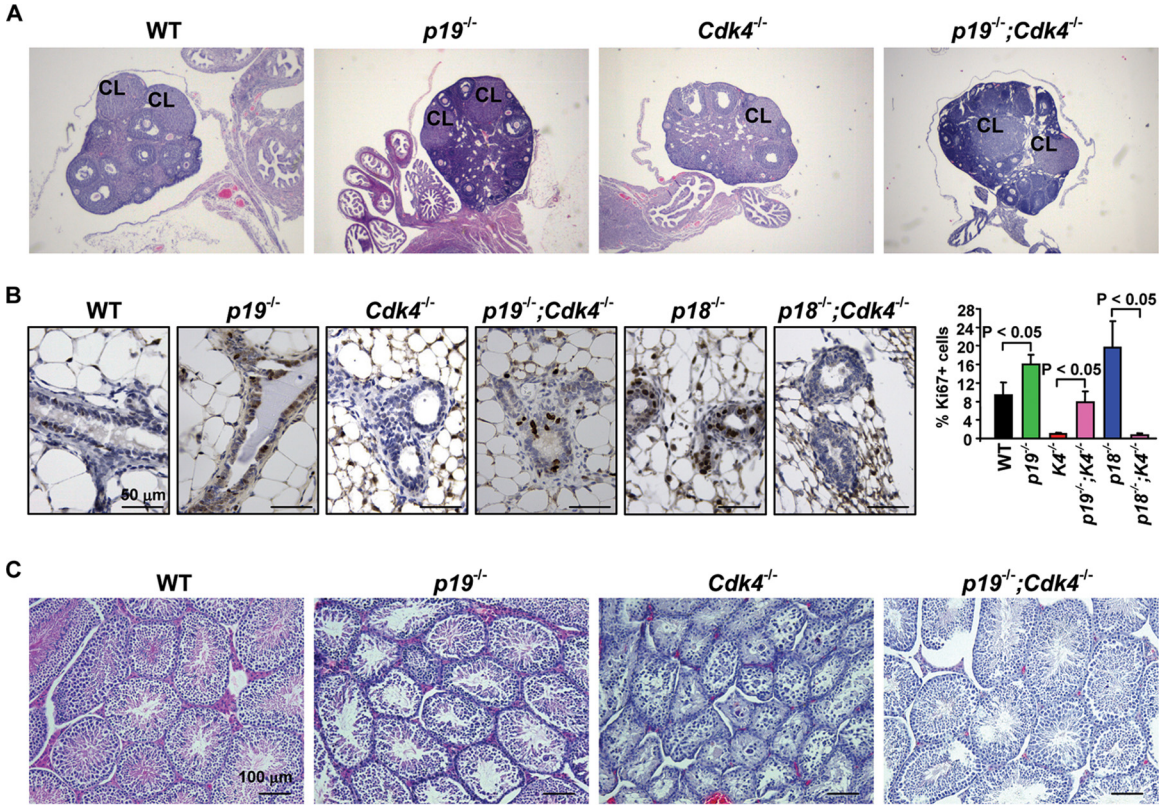

FIG 5 Loss of p19 rescues defective luteal function and MEC proliferation as well as infertility of Cdk4-deficient mice. (A and B) Ovaries (A) and mammary tissues (B) from mice of different genotypes at 4 months of age were stained with H&E and Ki67, respectively. The percentages of Ki67-positive cells were calculated from cells situated in clear ductal/glandular structures. Results represent the means ± SD of three animals per group. CL, corpus luteum. Statistical significance was calculated using Student's *t* test. (C) Testes from mice of different genotypes at 4 months of age were stained with H&E.

$p19^{-/-}$ female mice (6/10 mated with $p19^{-/-}$ and 7/10 mated with WT males) gave birth to an average of 6.5 and 7.8 pups within 21 days of males being introduced, respectively, which was slightly but not significantly lower than what occurred with WT females (90% pregnancy with an average of 9.2 pups [Table 2 and data not shown]). No $Cdk4^{-/-}$ female mice (0/10 mated with $Cdk4^{-/-}$ and 0/10 mated with WT males) became pregnant, whereas 67% (4/6) of $p19^{-/-}$; $Cdk4^{-/-}$ female mice mated with $p19^{-/-}$; $Cdk4^{-/-}$ males and 70% (7/10) of $p19^{-/-}$; $Cdk4^{-/-}$ female mice mated with WT males became pregnant and gave birth to an average of 6.2 and 6.9 pups, respectively, in a similar mating course, which is comparable to that of $p19^{-/-}$ female mice (Table 2). Together, these results confirmed that loss of *p19* rescued the infertility of Cdk4-deficient female mice.

TABLE 2 Fertility of mice

Mating pair	No. of pregnancies/ no. of pairs	Avg litter size
Female WT × male WT	9/10	9.2
Female $p19^{-/-}$ × male $p19^{-/-}$	6/10	6.5
Female $p19^{-/-}$ × male WT	7/10	7.8
Female WT × male $p19^{-/-}$	6/10	6.9
Female $Cdk4^{-/-}$ × male $Cdk4^{-/-}$	0/10	NA[a]
Female $Cdk4^{-/-}$ × male WT	0/10	NA
Female WT × male $Cdk4^{-/-}$	0/10	NA
Female $p19^{-/-}$; $Cdk4^{-/-}$ × male $p19^{-/-}$; $Cdk4^{-/-}$	4/6	6.2
Female $p19^{-/-}$; $Cdk4^{-/-}$ × male WT	7/10	6.9
Female WT × male $p19^{-/-}$; $Cdk4^{-/-}$	3/5	6.3

[a] NA, not applicable.

Due to defective PRL production from the pituitary and progesterone secretion from the CL of the ovary, $Cdk4^{-/-}$ female mice are unable to support embryo implantation (37, 50). Both PRL and progesterone are also essential for the proliferation and differentiation of the developing mammary gland (51). Since deletion of p19 rescued lactotroph hypoplasia and defective luteal function of $Cdk4^{-/-}$ mice, we expected to detect normal mammary development in $p19^{-/-}$; $Cdk4^{-/-}$ female mice. Indeed, $Cdk4^{-/-}$ mammary tissues, in line with the previous finding (52), showed a distinctive reduction in the number of mammary ducts with a significant decrease of mammary epithelial cell (MEC) proliferation compared with WT counterparts, as evidenced by Ki67 staining (Fig. 5B and data not shown). As expected, there were more Ki67-positive MECs in $p19^{-/-}$ mice than in WT mice. $p19^{-/-}$; $Cdk4^{-/-}$ mice displayed amounts of Ki67-positive MECs comparable to those of WT mice and significantly more Ki67-positive MECs than $Cdk4^{-/-}$ mice. These results suggest that the Cdk4 deficiency-induced proliferation defect in MECs is rescued by codeletion of p19, further confirming functional lactotrophs and CL in $p19^{-/-}$; $Cdk4^{-/-}$ mice.

As a comparison, we also performed side-by-side analysis of MEC proliferation in $p18^{-/-}$ and $p18^{-/-}$; $Cdk4^{-/-}$ mice. We

found that Ki67-positive MECs in $p18^{-/-}$; $Cdk4^{-/-}$ mice were indistinguishable from those of $Cdk4^{-/-}$ mice, though a robust increase of Ki67-positive MECs was detected in p18 null mice compared to WT (Fig. 5B), indicating that the function of p18 in suppressing MEC proliferation, unlike that of p19, is dependent on Cdk4. This result is in agreement with our previous finding that loss of p18 does not rescue pituitary hypoplasia and lactotroph dysfunction or the defective luteal function in Cdk4-deficient mice (21), which are the direct causes of female infertility and hypoproliferative MECs in $p18^{-/-}$; $Cdk4^{-/-}$ mice.

Taken together, these results indicate that Cdk4 is not required for female fertility or development of the ovaries and mammary glands in p19-deficient mice. Codeletion of p19 in Cdk4-deficient mice rescued lactotroph hypoplasia, resulting in normal luteal function, leading to female fertility with normal mammary gland development.

Deletion of *p19* rescues the infertility of *Cdk4* null male mice. All $Cdk4^{-/-}$ male mice tested failed to induce female pregnancy, and 60% of $p19^{-/-}$ male mice induced female pregnancy (6/10 mated with $p19^{-/-}$ and 6/10 mated with WT females), which was slightly but not significantly lower than for WT males (70% mated with $p19^{-/-}$ and 90% mated with WT females [Table 2]). Importantly, 60% to 67% of $p19^{-/-}$; $Cdk4^{-/-}$ male mice were able to induce female pregnancy (3/5 mated with WT and 4/6 mated with $p19^{-/-}$; $Cdk4^{-/-}$ females [Table 2]). Histology analysis revealed that while $Cdk4^{-/-}$ testes contained abnormal seminiferous tubules with degeneration of a significant fraction of primary spermatocytes and very few normal spermatozoa at an age of 4 months, testes from $p19^{-/-}$ and $p19^{-/-}$; $Cdk4^{-/-}$ mice displayed relatively normal seminiferous tubules compared with WT mice (Fig. 5C). These results suggest that deletion of p19 rescues testicular atrophy and infertility of male mice lacking Cdk4. It remains to be determined whether the rescue of hypoplasia in $Cdk4^{-/-}$ pituitaries by p19 loss contributes to the rescue of infertility of $Cdk4^{-/-}$ males, since we did not detect proliferation defects in FSH-expressing cells in $Cdk4^{-/-}$ and $p19^{-/-}$; $Cdk4^{-/-}$ pituitaries.

Loss of *p19* increases kinase activity of *Cdk4* and *Cdk6*, accelerating cell proliferation. Early-passage primary $p19^{-/-}$ MEFs proliferated faster than WT MEFs from the same litter at different passages (Fig. 6A). Consistently, BrdU pulse-labeling and flow cytometric analysis of asynchronously growing MEFs indicated that the $p19^{-/-}$ MEFs had decreased G_1- and increased S-phase cells relative to their WT counterparts (S-phase cells, 29.3% ± 3.2% versus 22.3% ± 2.1% [Fig. 6B]). Analysis of Rb protein in MEFs indicated that the level of total protein was reduced but the slower-migrating, hyperphosphorylated form was increased in $p19^{-/-}$ MEFs (Fig. 6C). Consistently, kinase activities of Cdk4 and Cdk6, the latter in particular, were enhanced in $p19^{-/-}$ MEFs compared to their WT counterparts (1.3-fold for Cdk4 and 2.0-fold for Cdk6 [Fig. 6D]), confirming the activation of Cdk4 and Cdk6 by p19 deficiency in MEFs. To test whether reduction of Rb protein was specifically caused by p19 loss and not due to secondary effects, we targeted *p19* mRNA in WT MEFs by RNA interference (RNAi). An effective suppression of p19 in MEFs was achieved as determined by both RT-PCR and immunoblotting (Fig. 6E and data not shown). The level of pRb protein in siRNA-targeted WT MEFs was also reduced, although not as much as in $p19^{-/-}$ MEFs (Fig. 6C and E). Transduction of p19 (Fig. 6F) and p16 (data not shown) retroviruses into $p19^{-/-}$ MEFs nearly completely inhibited DNA synthesis, indicating that $p19^{-/-}$ MEFs retained intact Rb and p107–p130 functions. The role of p19 in the negative regulation of S phase was consistent with its oscillating expression during the cell cycle: there was an accumulation of p19 in serum-deprived quiescent cells, which then fell sharply during G_1 after serum stimulation and accumulated again as cells progressed through the S phase (Fig. 6G). To further determine the function of p19 in the G_1-to-S transition, we examined the response of $p19^{-/-}$ MEFs to serum starvation. Compared to WT MEFs, deletion of p19 resulted in an accelerated progression through the G_1 phase and entry into S phase. While 15% and 25% of $p19^{-/-}$ MEFs had started DNA replication at 18 and 24 h post-serum stimulation, respectively, only 7% and 15% of WT MEFs were BrdU positive (Fig. 6H and I) at the same time points. Together, these results indicate that loss of p19 function increases the kinase activity of Cdk4 and Cdk6, particularly that of Cdk6, accelerating the G_1-to-S transition.

Loss of *p19* increases Cdk6 activity, rescuing S-phase delay in MEFs lacking *Cdk4*. The cell cycle kinetics of $p19^{-/-}$ MEFs in response to serum deprivation-stimulation was in contrast to that of $Cdk4^{-/-}$ MEFs, which as previously reported displayed a delayed entry into S phase relative to WT MEFs, but it was similar to that of $p18^{-/-}$ MEFs, which also displayed accelerated progression through the G_1 phase (21, 38, 49). To determine the functional interaction between CDK4 and p19, we generated $p19^{-/-}$; $Cdk4^{-/-}$ MEFs and determined their cell cycle kinetics in response to serum deprivation and stimulation. We found that $p19^{-/-}$; $Cdk4^{-/-}$ MEFs exhibited kinetics more similar to those of WT MEFs: 4% and 13% of cells were stained positive for BrdU at 18 and 24 h post-serum stimulation, respectively, which is significantly higher than for $Cdk4^{-/-}$ MEFs, where 1% and 7% of cells were BrdU positive at the same time points (Fig. 6H and I). These results indicate that *p19* plays a critical role in controlling the serum response in MEFs by regulating not only Cdk4 but also another target—likely Cdk6—and that a delay in S-phase entry by loss of *Cdk4* could be compensated by an increase of Cdk6 activity. These data are consistent with the findings derived *in vivo* indicating that loss of p19 rescues the hypoproliferative phenotypes associated with Cdk4 deficiency in the lactotroph.

Next, we determined Cdk6 activity using the ADP-Glo kinase assay kit and found that $p19^{-/-}$; $Cdk4^{-/-}$ MEFs displayed 1.3-fold more Cdk6 kinase activity than $Cdk4^{-/-}$ MEFs (Fig. 6J). To further consolidate the role of p19 in the regulation of kinase activity of Cdk4 and Cdk6, we developed a new assay. We immunoprecipitated Cdk4- and Cdk6-associated complexes from mouse thymus, which express high levels of both Cdk4 and Cdk6 (data not shown), and incubated the complex with a GST-Rb substrate in the presence of ATP. The reaction was terminated, and the results were analyzed by Western blotting with a phosphothreonine-specific antibody (P-Thr). We detected strong phosphorylated Rb bands induced by Cdk4- and Cdk6-associated complexes and a very faint band in the IgG control (Fig. 6K), validating this assay as an alternative means to determine Cdk4 and Cdk6 activity *in vitro*. We then immunoprecipitated Cdk4- and Cdk6-associated complexes from MEFs of different genotypes and detected greater phosphorylation of Rb in $p19^{-/-}$ MEFs than in WT fibroblasts (Fig. 6L, lanes 2 and 6 versus lanes 1 and 5, respectively). Compared to WT, the increased Cdk6-associated phosphorylation of Rb in $p19^{-/-}$ MEFs is more drastic than the Cdk4-associated phosphorylation of Rb. These results further confirm the enhancement of kinase activity of Cdk4 and Cdk6, particularly that

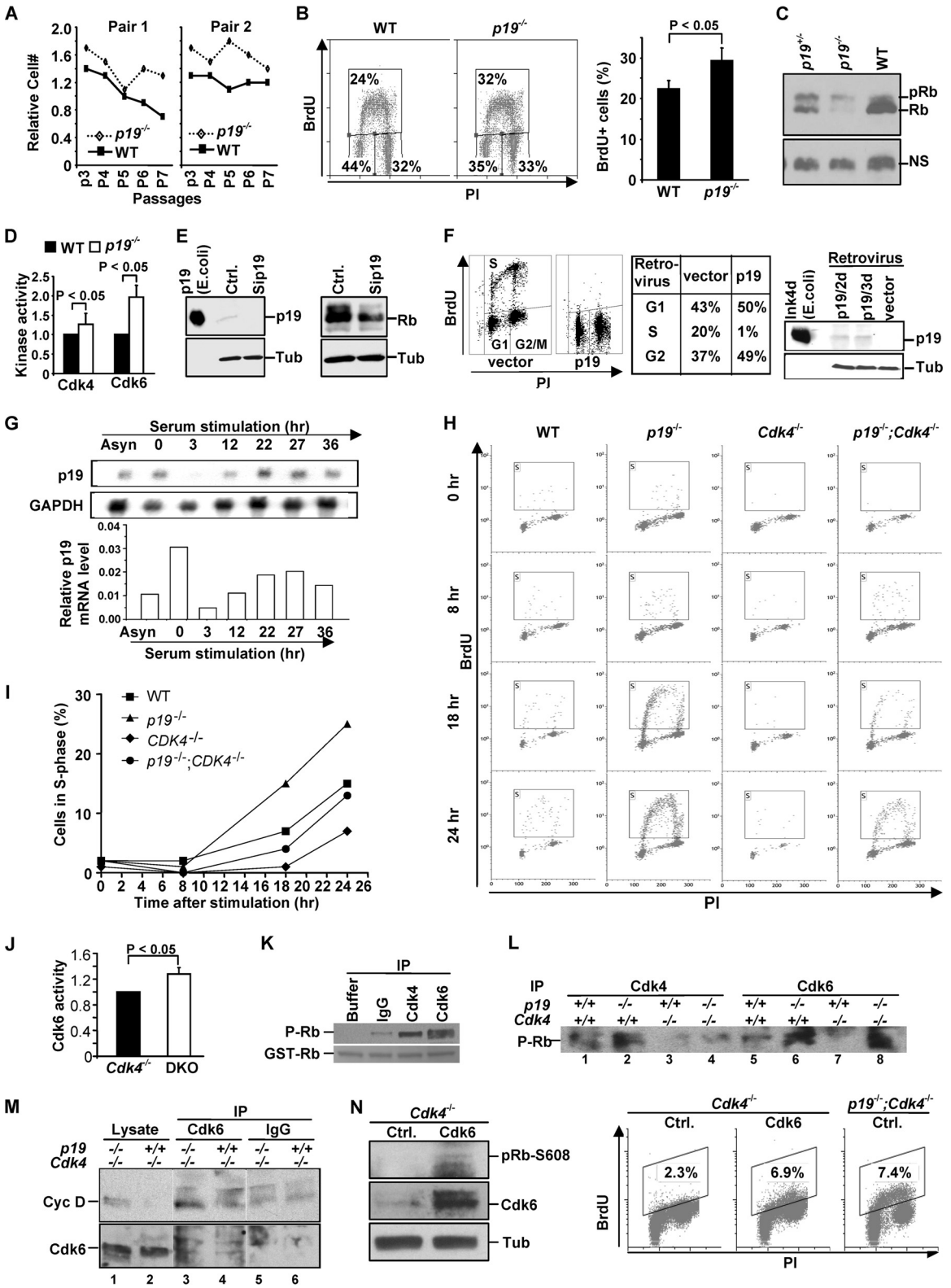

FIG 6 p19 controls proliferation of MEFs that is not dependent on Cdk4. (A) A total of 10^6 primary WT and $p19^{-/-}$ MEFs isolated from two separate litters were cultured on 100-mm dishes in duplicate on a 3T9 protocol for 7 passages. At 3-day intervals, the number of cells on each plate was determined prior to reseeding 10^6 cells per dish for the next passage. (B) Asynchronously growing MEFs derived from the littermate embryos at passage 1 were pulse-labeled with BrdU. Cells were stained with anti-BrdU antibody and propidium iodide (PI) and then analyzed by flow cytometry. The percentages of BrdU-positive (S-phase), G_1, and G_2 cells are shown. The average percentages of BrdU-positive cells were calculated from three different pairs of MEFs. (C) Asynchronously growing MEFs at early passages were collected and lysed, and the expression of pRb was examined by Western blotting. (D) Kinase activity associated with Cdk4 and Cdk6 in MEFs of

of Cdk6, by p19 loss in MEFs. Importantly, the Cdk6-associated Rb phosphorylation in *p19*$^{-/-}$; *Cdk4*$^{-/-}$ MEFs is significantly increased compared to *Cdk4*$^{-/-}$ MEFs (Fig. 6L, lane 8 versus lane 7), further confirming the increase of Cdk6 activity in *p19*$^{-/-}$; *Cdk4*$^{-/-}$ MEFs relative to *Cdk4*$^{-/-}$ MEFs. Consistent with these data, we detected more cyclin D coimmunoprecipitated with Cdk6 in *p19*$^{-/-}$; *Cdk4*$^{-/-}$ MEFs than in *Cdk4*$^{-/-}$ MEFs, though Cdk6 levels were comparable in these cells (Fig. 6M, lane 3 versus lane 4), indicating that loss of p19 stimulates binding of cyclin D to Cdk6 in Cdk4-deficient cells. Interestingly, we repeatedly detected more cyclin D in *p19*$^{-/-}$; *Cdk4*$^{-/-}$ MEFs than in *Cdk4*$^{-/-}$ MEFs (Fig. 6M, lanes 1 and 2), suggesting that loss of p19 in Cdk4-deficient MEFs also resulted in the increase of cyclin D protein level, the mechanism of which remains to be determined. We then transfected Cdk6 in *Cdk4*$^{-/-}$ MEFs and found that ectopic Cdk6 stimulated phosphorylation of Rb protein (Fig. 6N, left panel) and increased BrdU incorporation compared with control MEFs (6.9% versus 2.3% [Fig. 6N]). Furthermore, BrdU incorporation in *Cdk4*$^{-/-}$ MEFs overexpressing Cdk6 was comparable with that in *p19*$^{-/-}$; *Cdk4*$^{-/-}$ MEFs (6.9% versus 7.4% [Fig. 6N]), indicating that overexpression of Cdk6 is sufficient to drive *Cdk4*$^{-/-}$ MEFs into S phase with faster kinetics.

In sum, these results suggest that loss of p19 increases the kinase activity of Cdk6 by stimulating its binding with cyclin D, leading to rescue of S-phase delay in MEFs deficient for *Cdk4*.

DISCUSSION

p19 functions as a tumor suppressor. Mice lacking p19 developed widespread hyperplasia and spontaneous tumors, indicating a role of p19 in tumor suppression. Consistent with its broad expression (24), tumors spontaneously developed in *p19* mutant mice across a wide spectrum of at least 6 different organs or tissues. The mechanism underlying the tumor development induced by p19 loss is that loss of p19 function, like that of the other three members of Ink4 family cell cycle inhibitors, enhances the activity of Cdk4/6 and phosphorylation of Rb protein, leading to significantly increased cell proliferation and eventually tumor development.

Of the four Ink4 family members, p19 is the most highly and ubiquitously expressed in embryos and adult tissues (24). Biochemical properties of the individual INK4 members are almost indistinguishable (1, 2). However, loss of p15 confers proliferative advantage to MEFs and results in a moderate increase of tumor development, mostly sarcomas, in mice (11). p16 null mice develop sarcomas, lymphomas, and melanomas (10, 12), and p18 null mice develop widespread hyperplasia, organomegaly, and breast and pituitary IL tumors (11, 15). Our finding that deletion of p19 in mice leads to widespread tumor development is in agreement with the observation that loss of p19 expression is frequently detected in human cancers (25, 26). The broad and distinct expression patterns of INK4 members as well as diverse phenotypes of the mice lacking individual *Ink4* genes further support a model that *INK4* genes collaboratively suppress tumor development *in vivo*.

Previous analyses of mice harboring a different mutant *p19* allele, *p19*^{tm1Maro}, containing an insertion of *LacZ-Neo*^{r}, demonstrated a relatively minor phenotype of testicular atrophy and no tumor phenotype (28). The discrepant results from two different mutant *p19* alleles are likely caused by the use of mice with different genetic backgrounds as well as different targeting strategies, in which we deleted the entire *p19* gene from the genome without insertion of exogenous genes. Four lines of evidence collectively support that the tumorigenic and cellular phenotypes described in our study are caused by the loss of p19 function. First, all hyperplastic and tumorigenic phenotypes observed in our p19 null mice have been previously described in mice that lack individual or a combination of *Rb* genes or harbor an Ink4-resistant mutation of *Cdk4* (2, 4–7, 39, 53, 54). Second, the pattern of *p19* gene expression is consistent with the phenotypes observed in null MEFs: accelerated G_1-to-S transition. In cultured cells, the levels of p19 mRNA and protein oscillate during the cell cycle, accumulating in quiescent cells, falling sharply during G_1 phase, and accumulating again as cells progress through the S phase (Fig. 6 and reference 55). Third, p19 null MEFs and cells in multiple organs are highly proliferative, with a concomitant increase of Cdk4/6 activity and Rb protein phosphorylation at a Cdk4/6-specific site, consistent with the notion that *INK4* genes function as upstream activators of Rb protein through the inhibition of Cdk4/6. Fourth, knockdown of p19 in WT MEFs, like *p19*$^{-/-}$ MEFs, also led to a decreased level of Rb protein (Fig. 6E), and that transduction of WT

different genotypes. Results represent the means ± SD from triplicates of representative MEFs generated from littermate embryos. (E) WT MEFs at passage 1 were transfected with either single-stranded sense RNA oligonucleotides or siRNA duplex targeting p19. The expression of p19 and Rb was determined by Western analysis. (F) *p19*$^{-/-}$ MEFs were infected with a retrovirus expressing p19 or empty vector. Forty-eight hours after infection, cells were pulse-labeled with BrdU for 4 h and analyzed by flow cytometry. p19 expression was verified by Western blotting of total cell lysates prepared 24 h and 48 h after infection. (G) WT MEFs were serum deprived for 3 days and released from quiescence by serum stimulation. Total RNA was prepared from cells at different time points after serum stimulation as well as from an asynchronized cell population as indicated. RNA samples were resolved on a 1% agarose gel, transferred to a nitrocellulose filter, and hybridized with a probe derived from full-length mouse *p19* cDNA. The blot was then stripped and rehybridized with a mouse GAPDH probe. The amount of *p19* mRNA at each time point of the Northern blot was normalized by GAPDH and plotted (bottom panel). (H) MEFs of different genotypes were starved for 72 h (time zero), followed by stimulation of cells with medium containing 10% serum. Cells were pulse-labeled with BrdU and harvested at the times indicated after stimulation. Cells were stained with anti-BrdU antibody and PI and then analyzed by flow cytometry. BrdU-positive cells are marked by a box. (I) The percentage of cells in S phase from each time point in panel H was plotted. Results represent one of three independent experiments from three independent *p19*$^{-/-}$; *Cdk4*$^{-/-}$ and *Cdk4*$^{-/-}$ MEFs and two independent WT and *p19*$^{-/-}$ MEFs. (J) Kinase activity associated with Cdk6 in MEFs of different genotypes. Results represent the means ± SD from triplicates of representative MEFs generated from littermate embryos. (K) Lysate from 6-week-old mouse thymus was precipitated with antibodies against Cdk4 and Cdk6 or with rabbit IgG and buffer as negative controls. Immunoprecipitates were reacted with GST-Rb in the presence of ATP, separated electrophoretically, and immunoblotted with a phosphothreonine-specific antibody. Phosphorylated Rb (P-Rb) and Ponceau-stained GST-Rb are shown. (L) Lysates from MEFs of different genotypes were precipitated with antibodies against Cdk4 or Cdk6. Immunoprecipitates were reacted with GST-Rb in the presence of ATP and immunoblotted with a phosphothreonine-specific antibody. (M) Lysates from MEFs of different genotypes were precipitated with antibodies against Cdk6 or rabbit IgG. Immunoprecipitates were immunoblotted with antibodies against Cdk6 or Cyc D (mixture of Cyc D1, D2, and D3). (N) *Cdk4*$^{-/-}$ MEFs at passage 4 were transfected with pCMV-Cdk6 (Cdk6) or pCMV-empty (Ctrl) for 2 days, and the cells were lysed for Western blotting (left panel) or pulse-labeled with BrdU for flow cytometry analysis with anti-BrdU antibody and PI (right panel). BrdU-positive cells are marked by a box. *p19*$^{-/-}$; *Cdk4*$^{-/-}$ MEFs at passage 4 transfected with pCMV-empty (Ctrl.) in parallel were also analyzed by flow cytometry as a control.

p19 in $p19^{-/-}$ MEFs nearly completely inhibited DNA synthesis (Fig. 6F).

To address the possibility that the expression of a gene(s) closely linked to *p19* was inadvertently affected in our mutant mice, we determined the mRNA levels of two genes neighboring the *p19* locus, one from each adjacent side, by qRT-PCR. No discernible change of mRNA level was seen in any of these genes. While we cannot exclude the possibility that one of these *p19* neighboring genes endured a subtle change in spatial or temporary expression beyond our detection sensitivity or that the expression of a gene at a greater distance from the *p19* locus might have been inadvertently affected in our mutant, we consider the probability of such an event occurring, and thus contributing to the observed phenotype, to be exceedingly low.

Function of p19 in controlling pituitary AL cell proliferation. In this paper, we provide compelling genetic evidence that p19 plays a critical role in suppressing pituitary AL cell proliferation. We discovered that deletion of *p19* in mice stimulates Cdk4 and Cdk6 activity toward Rb protein in pituitary AL cells, increasing their proliferation, particularly of lactotrophs, at an early age and eventually leading to hyperplasia and spontaneous tumor development. Loss of p19 rescues pituitary AL hypoplasia caused by Cdk4 deficiency, and loss of Cdk4 does not abolish the hyperproliferative phenotype in $p19^{-/-}$ pituitaries, suggesting that development of a hyperproliferative phenotype in $p19^{-/-}$ pituitaries does not require Cdk4. We demonstrated that loss of p19 leads to phosphorylation of Rb in $Cdk4^{-/-}$ pituitary AL cells, likely through the activation of Cdk6. These results, together with previous findings derived from *p15*, *p16*, *p18*, *p21*, *p27*, and *p57* mutant mice (8–17), suggest that *p19* is the major CKI gene that controls pituitary AL cell proliferation.

Most pituitary hormones are produced in the AL, and most human pituitary tumors are AL tumors that express and secrete several hormones that contribute to various endocrine syndromes (34). In this study, we show that loss of Cdk4 alone, as reported (37, 38), does not induce a compensatory increase of Cdk6 in the pituitary, leading to defective cell proliferation. However, Cdk6 plays a significant role in regulating $p19^{-/-}$; $Cdk4^{-/-}$ cell proliferation in the pituitary AL, either in its own right or induced in a compensatory manner after Cdk4 loss, thereby sensitizing cells to p19 loss. Consistent with these findings were the observations that both p19 and Cdk6 are predominantly expressed in pituitary AL and that deletion of *p19* increases Cdk6 activity in the pituitary (Fig. 2D and 3 and reference 40). Nearly all $Cdk4^{-/-}$ mice died of diabetes early in life, with tiny pituitaries (Fig. 3 and 4), which prevented us from obtaining enough pituitaries from $Cdk4^{-/-}$ mice to directly confirm the increase of Cdk6 activity in $p19^{-/-}$; $Cdk4^{-/-}$ pituitaries in comparison to $Cdk4^{-/-}$ pituitaries. Notably, Cdk6 is readily detectable in MEFs (38), like in pituitary AL cells, and the loss of p19 significantly increases the kinase activity of Cdk6 as well as rescues the delay of G_1-to-S progression of $Cdk4^{-/-}$ MEFs following serum deprivation and stimulation (Fig. 6H, I, J, and L)—the key cellular defect caused by Cdk4 loss—supporting the role of Cdk6 in controlling G_1 progression of $p19^{-/-}$; $Cdk4^{-/-}$ cells. The findings that loss of p19 stimulates binding of cyclin D to Cdk6 in Cdk4-deficient MEFs and that ectopic expression of Cdk6 is sufficient to drive $Cdk4^{-/-}$ cells into S phase with faster kinetics further confirm that in the absence of Cdk4, p19 contributes to the failure of cells to enter S phase by preventing Cdk6 activation. Still, the *in vivo* function of Cdk6 systemically in the whole body and the manner in which Cdk6 compensates Cdk4 loss in different cell types and tissues remain unclear. However, the findings that Cdk6 is expressed at a very low level and does not compensate for Cdk4 loss in the pancreas (38) and that *Cdk4* loss cancels the pancreatic islet phenotype caused by *p19* loss but does not affect p19 deficiency defects in the pituitary suggest that Cdk6 plays an important role *in vivo* in mediating the function of p19 in a tissue-specific manner.

Defective PRL production in the $Cdk4^{-/-}$ pituitary AL is the cause of CL defects that then lead to defective progesterone secretion and female infertility (37, 50). We found that $p19^{-/-}$; $Cdk4^{-/-}$, but not $p18^{-/-}$; $Cdk4^{-/-}$, female mice are fertile with hyperproliferative lactotrophs as well as normal ovary CL formation and MEC proliferation (this study and reference 21), indicating that loss of p19 but not p18 in $Cdk4^{-/-}$ mice rescues lactotroph hypoplasia, resulting in normal luteal function and leading to female fertility with normal MEC proliferation. These results not only suggest a functional dependency of p18 and independency of p19 on Cdk4 in controlling pituitary cell proliferation but also confirm that lactotroph dysfunction is responsible for Cdk4-deficient female infertility and defective MEC proliferation.

Most, if not all, $Cdk4^{-/-}$ male mice are sterile, with impaired spermatogenesis (38, 49), which is also rescued by loss of p19 but not by loss of p18 (21). Due to the extremely low levels of Cdk6 protein expressed in WT testes (18, 38), it is unlikely that Cdk6 plays a critical role in regulating spermatogenesis of $p19^{-/-}$; $Cdk4^{-/-}$ mice. Diabetes-associated sterility has been documented in diabetic patients and animals (56, 57), and sterility of $Cdk4^{-/-}$ male mice may also be caused by their diabetic phenotype (49). However, our results that $p19^{-/-}$; $Cdk4^{-/-}$ male mice are fertile but also develop diabetes and that $p18^{-/-}$; $Cdk4^{-/-}$ mice are sterile and have diabetes (21) suggest that male sterility in $Cdk4^{-/-}$ mice is not a result of diabetes but is very likely—at least partially—caused by pituitary hypoplasia. How pituitary hypoplasia in $Cdk4^{-/-}$ male mice induces their sterility remains to be determined.

ACKNOWLEDGMENTS

This project was initiated at the Department of Biochemistry and Biophysics, University of North Carolina at Chapel Hill. We thank Yue Xiong for his invaluable support, discussion, and critical reading of the manuscript, Beverly H. Koller and Anne Latour for assistance in gene targeting and generation of mutant mice, and the DVR core facility at the University of Miami for animal husbandry.

This study was supported in part by a DOD Idea Award (W81XWH-10-1-0302), the Braman Family Breast Cancer Institute of the University of Miami Sylvester Cancer Center, and startup funds from the University of Miami Miller School of Medicine to Xin-Hai Pei.

REFERENCES

1. **Pei XH, Xiong Y.** 2005. Biochemical and cellular mechanisms of mammalian CDK inhibitors: a few unresolved issues. Oncogene **24:**2787–2795. http://dx.doi.org/10.1038/sj.onc.1208611.
2. **Sherr CJ, McCormick F.** 2002. The RB and p53 pathways in cancer. Cancer Cell **2:**103–112. http://dx.doi.org/10.1016/S1535-6108(02)00102-2.
3. **Weinberg RA.** 1995. The retinoblastoma protein and cell cycle control. Cell **81:**323–330. http://dx.doi.org/10.1016/0092-8674(95)90385-2.
4. **Jacks T, Fazeli A, Schmitt EM, Bronson RT, Goodell MA, Weinberg RA.** 1992. Effects of an Rb mutation in the mouse. Nature **359:**295–300. http://dx.doi.org/10.1038/359295a0.
5. **Lee Y-HP, Chang C-Y, Hu N, Wang Y-CJ, Lai C-C, Herrup K, Lee W-H, Bradley A.** 1992. Mice deficient for Rb are nonviable and show defects in

neurogenesis and haematopoiesis. Nature **359:**288–294. http://dx.doi.org/10.1038/359288a0.
6. **Nikitin AY, Juarez-Perez MI, Li S, Huang L, Lee WH.** 1999. RB-mediated suppression of spontaneous multiple neuroendocrine neoplasia and lung metastases in Rb+/− mice. Proc. Natl. Acad. Sci. U. S. A. **96:**3916–3921. http://dx.doi.org/10.1073/pnas.96.7.3916.
7. **Williams BO, Schmitt EM, Remington L, Bronson RT, Albert DM, Weinberg RA, Jacks T.** 1994. Extensive contribution of Rb-deficient cells to adult chimeric mice with limited histopathological consequences. EMBO J. **13:**4251–4259.
8. **Brugarolas J, Chandrasekaran C, Gordon JI, Beach D, Jacks T, Hannon GJ.** 1995. Radiation-induced cell cycle arrest compromised by p21 deficiency. Nature **377:**552–557. http://dx.doi.org/10.1038/377552a0.
9. **Deng C, Zhang P, Harper JW, Elledge SJ, Leder P.** 1995. Mice lacking p21CIP1/WAF1 undergo normal development, but are defective in G1 checkpoint control. Cell **82:**675–684. http://dx.doi.org/10.1016/0092-8674(95)90039-X.
10. **Krimpenfort P, Quon KC, Mooi WJ, Loonstra A, Berns A.** 2001. Loss of $p16^{Ink4a}$ confers susceptibility to metastatic melanoma in mice. Nature **413:**83–86. http://dx.doi.org/10.1038/35092584.
11. **Latres E, Malumbres M, Sotillo R, Martin J, Ortega S, Martin-Caballero J, Flores JM, Cordon-Cardo C, Barbacid M.** 2000. Limited overlapping roles of P15(INK4b) and P18(INK4c) cell cycle inhibitors in proliferation and tumorigenesis. EMBO J. **19:**3496–3506. http://dx.doi.org/10.1093/emboj/19.13.3496.
12. **Sharpless NE, Bardeesy N, Lee KH, Carrasco D, Castrillon DH, Aguirre AJ, Wu EA, Horner JW, DePinho RA.** 2001. Loss of $p16^{Ink4a}$ with retention of $p19^{Arf}$ predisposes mice to tumorigenesis. Nature **413:**86–91. http://dx.doi.org/10.1038/35092592.
13. **Zhang P, Liegeois N, Wong C, Finegold M, Hou H, Thompson JC, Silverman A, Harper JW, DePinho RA, Elledge SJ.** 1997. Altered cell differentiation and proliferation in mice lacking $p57^{KIP2}$ indicates a role in Beckwith-Wiedemann syndrome. Nature **387:**151–158. http://dx.doi.org/10.1038/387151a0.
14. **Fero ML, Rivkin M, Tasch M, Porter P, Carow CE, Firpo E, Polyak K, Tsai LH, Broudy V, Perlmutter RM, Kaushansky K, Roberts JM.** 1996. A syndrome of multiorgan hyperplasia with features of gigantism, tumorigenesis, and female sterility in p27(Kip1)-deficient mice. Cell **85:**733–744. http://dx.doi.org/10.1016/S0092-8674(00)81239-8.
15. **Franklin DS, Godfrey VL, Lee H, Kovalev GI, Schoonhoven R, Chen-Kiang S, Su L, Xiong Y.** 1998. CDK inhibitors p18(INK4c) and p27(Kip1) mediate two separate pathways to collaboratively suppress pituitary tumorigenesis. Genes Dev. **12:**2899–2911. http://dx.doi.org/10.1101/gad.12.18.2899.
16. **Kiyokawa H, Kineman RD, Manova-Todorova KO, Soares VC, Hoffman ES, Ono M, Khanam D, Hayday AC, Frohman LA, Koff A.** 1996. Enhanced growth of mice lacking the cyclin-dependent kinase inhibitor function of p27(Kip1). Cell **85:**721–732. http://dx.doi.org/10.1016/S0092-8674(00)81238-6.
17. **Nakayama K, Ishida N, Shirane M, Inomata A, Inoue T, Shishido N, Horii I, Loh DY.** 1996. Mice lacking p27(Kip1) display increased body size, multiple organ hyperplasia, retinal dysplasia, and pituitary tumors. Cell **85:**707–720. http://dx.doi.org/10.1016/S0092-8674(00)81237-4.
18. **Zindy F, den Besten W, Chen B, Rehg JE, Latres E, Barbacid M, Pollard JW, Sherr CJ, Cohen PE, Roussel MF.** 2001. Control of spermatogenesis in mice by the cyclin D-dependent kinase inhibitors p18(Ink4c) and p19(Ink4d). Mol. Cell. Biol. **21:**3244–3255. http://dx.doi.org/10.1128/MCB.21.9.3244-3255.2001.
19. **Thullberg M, Bartkova J, Khan S, Hansen K, Ronnstrand L, Lukas J, Strauss M, Bartek J.** 2000. Distinct versus redundant properties among members of the INK4 family of cyclin-dependent kinase inhibitors. FEBS Lett. **470:**161–166. http://dx.doi.org/10.1016/S0014-5793(00)01307-7.
20. **Franklin DS, Godfrey VL, O'Brien DA, Deng C, Xiong Y.** 2000. Functional collaboration between different cyclin-dependent kinase inhibitors suppresses tumor growth with distinct tissue specificity. Mol. Cell. Biol. **20:**6147–6158. http://dx.doi.org/10.1128/MCB.20.16.6147-6158.2000.
21. **Pei XH, Bai F, Tsutsui T, Kiyokawa H, Xiong Y.** 2004. Genetic evidence for functional dependency of p18Ink4c on Cdk4. Mol. Cell. Biol. **24:**6653–6664. http://dx.doi.org/10.1128/MCB.24.15.6653-6664.2004.
22. **Ramsey MR, Krishnamurthy J, Pei XH, Torrice C, Lin W, Carrasco DR, Ligon KL, Xiong Y, Sharpless NE.** 2007. Expression of p16Ink4a compensates for p18Ink4c loss in cyclin-dependent kinase 4/6-dependent tumors and tissues. Cancer Res. **67:**4732–4741. http://dx.doi.org/10.1158/0008-5472.CAN-06-3437.
23. **Ruas M, Peters G.** 1998. The $p16^{INK4a}$/CDK2A tumor suppresor and its relatives. Biochim. Biophys. Acta **1378:**F115–F177.
24. **Zindy F, Quelle DE, Roussel MF, Sherr CJ.** 1997. Expression of the p16INK4a tumor suppressor versus other INK4 family members during mouse development and aging. Oncogene **15:**203–211. http://dx.doi.org/10.1038/sj.onc.1201178.
25. **Morishita A, Gong J, Deguchi A, Tani J, Miyoshi H, Yoshida H, Himoto T, Yoneyama H, Mori H, Kato K, Kurokohchi K, Deguchi K, Izuishi K, Suzuki Y, Kushida Y, Haba R, Iwama H, Watanabe S, D'Armiento J, Masaki T.** 2011. Frequent loss of p19INK4D expression in hepatocellular carcinoma: relationship to tumor differentiation and patient survival. Oncol. Rep. **26:**1363–1368. http://dx.doi.org/10.3892/or.2011.1452.
26. **Bartkova J, Thullberg M, Rajpert-De Meyts E, Skakkebaek NE, Bartek J.** 2000. Lack of p19INK4d in human testicular germ-cell tumours contrasts with high expression during normal spermatogenesis. Oncogene **19:**4146–4150. http://dx.doi.org/10.1038/sj.onc.1203769.
27. **Buchold GM, Magyar PL, O'Brien DA.** 2007. Mice lacking cyclin-dependent kinase inhibitor p19Ink4d show strain-specific effects on male reproduction. Mol. Reprod. Dev. **74:**1008–1020. http://dx.doi.org/10.1002/mrd.20715.
28. **Zindy F, van Deursen J, Grosveld G, Sherr CJ, Roussel MF.** 2000. INK4d-deficient mice are fertile despite testicular atrophy. Mol. Cell. Biol. **20:**372–378. http://dx.doi.org/10.1128/MCB.20.1.372-378.2000.
29. **Asa SL, Ezzat S.** 2002. The pathogenesis of pituitary tumours. Nat. Rev. Cancer **2:**836–849. http://dx.doi.org/10.1038/nrc926.
30. **Bamberger CM, Fehn M, Bamberger AM, Ludecke DK, Beil FU, Saeger W, Schulte HM.** 1999. Reduced expression levels of the cell-cycle inhibitor p27Kip1 in human pituitary adenomas. Eur. J. Endocrinol. **140:**250–255. http://dx.doi.org/10.1530/eje.0.1400250.
31. **Hossain MG, Iwata T, Mizusawa N, Qian ZR, Shima SW, Okutsu T, Yamada S, Sano T, Yoshimoto K.** 2009. Expression of p18(INK4C) is down-regulated in human pituitary adenomas. Endocr. Pathol. **20:**114–121. http://dx.doi.org/10.1007/s12022-009-9076-0.
32. **Lidhar K, Korbonits M, Jordan S, Khalimova Z, Kaltsas G, Lu X, Clayton RN, Jenkins PJ, Monson JP, Besser GM, Lowe DG, Grossman AB.** 1999. Low expression of the cell cycle inhibitor p27Kip1 in normal corticotroph cells, corticotroph tumors, and malignant pituitary tumors. J. Clin. Endocrinol. Metab. **84:**3823–3830. http://dx.doi.org/10.1210/jc.84.10.3823.
33. **Pei L, Melmed S, Scheithauer B, Kovacs K, Benedict WF, Prager D.** 1995. Frequent loss of heterozygosity at the retinoblastoma susceptibility gene (RB) locus in aggressive pituitary tumors: evidence for a chromosome 13 tumor suppressor gene other than RB. Cancer Res. **55:**1613–1616.
34. **Quereda V, Malumbres M.** 2009. Cell cycle control of pituitary development and disease. J. Mol. Endocrinol. **42:**75–86. http://dx.doi.org/10.1677/JME-08-0146.
35. **Woloschak M, Yu A, Post KD.** 1997. Frequent inactivation of the p16 gene in human pituitary tumors by gene methylation. Mol. Carcinog. **19:**221–224. http://dx.doi.org/10.1002/(SICI)1098-2744(199708)19:4<221::AID-MC1>3.0.CO;2-F.
36. **Jirawatnotai S, Aziyu A, Osmundson EC, Moons DS, Zou X, Kineman RD, Kiyokawa H.** 2004. Cdk4 is indispensable for postnatal proliferation of the anterior pituitary. J. Biol. Chem. **279:**51100–51106. http://dx.doi.org/10.1074/jbc.M409080200.
37. **Moons DS, Jirawatnotai S, Parlow AF, Gibori G, Kineman RD, Kiyokawa H.** 2002. Pituitary hypoplasia and lactotroph dysfunction in mice deficient for cyclin-dependent kinase-4. Endocrinology **143:**3001–3008. http://dx.doi.org/10.1210/en.143.8.3001.
38. **Tsutsui T, Hesabi B, Moons DS, Pandolfi PA, Hansel KS, Koff A, Kiyokawa H.** 1999. Targeted disruption of CDK4 delays cell cycle entry with enhanced $p27^{Kip1}$ activity. Mol. Cell. Biol. **19:**7011–7019.
39. **Sotillo R, Dubus P, Martin J, de La Cueva E, Ortega S, Malumbres M, Barbacid M.** 2001. Wide spectrum of tumors in knock-in mice carrying a Cdk4 protein insensitive to INK4 inhibitors. EMBO J. **20:**6637–6647. http://dx.doi.org/10.1093/emboj/20.23.6637.
40. **Buchold GM, Magyar PL, Arumugam R, Lee MM, O'Brien DA.** 2007. p19Ink4d and p18Ink4c cyclin-dependent kinase inhibitors in the male reproductive axis. Mol. Reprod. Dev. **74:**997–1007. http://dx.doi.org/10.1002/mrd.20716.
41. **Franklin DS, Xiong Y.** 1996. Induction of p18INK4c and its predominant

association with CDK4 and CDK6 during myogenic differentiation. Mol. Biol. Cell **7:**1587–1599. http://dx.doi.org/10.1091/mbc.7.10.1587.
42. **Phelps DE, Xiong Y.** 1998. Regulation of cyclin-dependent kinase 4 during adipogenesis involves switching of cyclin D subunits and concurrent binding of p18INK4c and p27Kip1. Cell Growth Differ. **9:**595–610.
43. **Xiong Y, Zhang H, Beach D.** 1993. Subunit rearrangement of cyclin-dependent kinases is associated with cellular transformation. Genes Dev. **7:**1572–1583. http://dx.doi.org/10.1101/gad.7.8.1572.
44. **Pei XH, Bai F, Li Z, Smith MD, Whitewolf G, Jin R, Xiong Y.** 2011. Cytoplasmic CUL9/PARC ubiquitin ligase is a tumor suppressor and promotes p53-dependent apoptosis. Cancer Res. **71:**2969–2977. http://dx.doi.org/10.1158/0008-5472.CAN-10-4300.
45. **Jenkins CW, Xiong Y.** 1995. Immunoprecipitation and immunoblotting in cell cycle studies, p 250–263. *In* Pagano M (ed), Cell cycle: material and methods. Springer-Verlag, New York, NY.
46. **Burke JR, Hura GL, Rubin SM.** 2012. Structures of inactive retinoblastoma protein reveal multiple mechanisms for cell cycle control. Genes Dev. **26:**1156–1166. http://dx.doi.org/10.1101/gad.189837.112.
47. **Schmitz NM, Leibundgut K, Hirt A.** 2004. MCM4 shares homology to a replication/DNA-binding domain in CTF and is contacted by pRb. Biochem. Biophys. Res. Commun. **317:**779–786. http://dx.doi.org/10.1016/j.bbrc.2004.03.109.
48. **Zarkowska T, Harlow SUE, Mittnacht S.** 1997. Monoclonal antibodies specific for underphosphorylated retinoblastoma protein identify a cell cycle regulated phosphorylation site targeted by CDKs. Oncogene **14:**249–254. http://dx.doi.org/10.1038/sj.onc.1200824.
49. **Rane SG, Dubus P, Mettus R, Galvreath EJ, Boden G, Reddy EP, Barbacid M.** 1999. Loss of Cdk4 expression causes insulin-deficient diabetes and Cdk4 activatiion results in b-islet cell hyperplasia. Nat. Genet. **22:**44–52. http://dx.doi.org/10.1038/8751.
50. **Moons DS, Jirawatnotai S, Tsutsui T, Franks R, Parlow AF, Hales DB, Gibori G, Fazleabas AT, Kiyokawa H.** 2002. Intact follicular maturation and defective luteal function in mice deficient for cyclin-dependent kinase-4. Endocrinology **143:**647–654. http://dx.doi.org/10.1210/en.143.2.647.
51. **Lee HJ, Ormandy CJ.** 2012. Interplay between progesterone and prolactin in mammary development and implications for breast cancer. Mol. Cell. Endocrinol. **357:**101–107. http://dx.doi.org/10.1016/j.mce.2011.09.020.
52. **Reddy HK, Mettus RV, Rane SG, Grana X, Litvin J, Reddy EP.** 2005. Cyclin-dependent kinase 4 expression is essential for neu-induced breast tumorigenesis. Cancer Res. **65:**10174–10178. http://dx.doi.org/10.1158/0008-5472.CAN-05-2639.
53. **Hu N, Gutsmann A, Herbert DC, Bradley A, Lee W-H, Lee EY-HP.** 1994. Heterozygous *Rb*-1^{D20}/+ mice are predisposed to tumors of the pituitary gland with a nearly complete penetrance. Oncogene **9:**1021–1027.
54. **Maandag EC, Van Der Valk M, Vlaar M, Feltkamp C, O'Brien J, Van Roon M, Van Der Lugt N, Berns A, Te Riele H.** 1994. Developmental rescue of an embryonic-lethal mutation in the retinoblastoma gene in chimeric mice. EMBO J. **13:**4260–4268.
55. **Thullberg M, Bartek J, Lukas J.** 2000. Ubiquitin/proteasome-mediated degradation of p19^{INK4d} determines its periodic expression during the cell cycle. Oncogene **19:**2870–2875. http://dx.doi.org/10.1038/sj.onc.1203579.
56. **Cameron DF, Murray FT, Drylie DD.** 1985. Interstitial compartment pathology and spermatogenic disruption in testes from impotent diabetic men. Anat. Rec. **213:**53–62. http://dx.doi.org/10.1002/ar.1092130108.
57. **Murray FT, Cameron DF, Orth JM.** 1983. Gonadal dysfunction in the spontaneously diabetic BB rat. Metabolism **32:**141–147. http://dx.doi.org/10.1016/S0026-0495(83)80028-6.